Discovery, Synthesis, and Structure Activity of a Highly Selective α7 Nicotinic Acetylcholine Receptor Antagonist†

Paul Whiteaker,*,‡ Sean Christensen,§ Doju Yoshikami,§ Cheryl Dowell,§ Maren Watkins,§ Jozsef Gulyas,|| Jean Rivier,|| Baldomero M. Olivera,§ and J. Michael McIntosh§,⊥

Institute for Behavioral Genetics, University of Colorado, Boulder, Colorado 80309, Departments of Biology and Psychiatry, University of Utah, Salt Lake City, Utah 84112, and Clayton Foundation Laboratories for Peptide Biology, The Salk Institute, La Jolla, California 92037

Received March 1, 2007; Revised Manuscript Received April 4, 2007

ABSTRACT: Nicotinic acetylcholine receptors (nAChRs) that contain an α7 subunit are widely distributed in neuronal and nonneuronal tissue. These receptors are implicated in the release of neurotransmitters such as glutamate and in functions ranging from thought processing to inflammation. Currently available ligands for α7 nAChRs have substantial affinity for one or more other nAChR subtypes, including those with an α1, α3, α6, and/or α9 subunit. An α-conotoxin gene was cloned from *Conus arenatus*. Predicted peptides were synthesized and found to potently block α3-, α6-, and α7-containing nAChRs. Structure−activity information regarding conotoxins from distantly related *Conus* species was employed to modify the *C. arenatus* derived toxin into a novel, highly selective α7 nAChR antagonist. This ligand, α-CtxArIB-[V11L,V16D], has low nanomolar affinity for rat α7 homomers expressed in *Xenopus laevis* oocytes, and antagonism is slowly reversible. Kinetic analysis provided insight into the mechanism of antagonism. α-CtxArIB interacts with five ligand binding sites per α7 receptor, and occupation of a single site is sufficient to block function. The peptide was also shown to be highly selective in competition binding assays in rat brain membranes. α-CtxArIB[V11L,V16D] is the most selective ligand yet reported for α7 nAChRs.

Nicotinic acetylcholine receptors (nAChRs)[1] are expressed throughout the mammalian central nervous system and are pentameric assemblies of homologous subunits. Neuronal nAChRs are mainly presynaptic and primarily function by modulating the release of a wide range of neurotransmitters (*1*). To date, 11 mammalian neuronal subunit genes have been identified, α2−α7, α9, α10, and *β*2−*β*4 (α8 is apparently only expressed in avian neurons), with overlapping expression patterns (*2*). Different subunit combinations produce different nAChR subtypes. As might be anticipated given the extensive sequence homology among subunits, it is difficult to distinguish subtypes pharmacologically.

α-Bungarotoxin (α-Bgt), a peptide neurotoxin from the venom of the Taiwanese banded krait *Bungarus multicinctus*, was first used to identify and characterize the muscle-type nAChR. Later, [^{125}I]α-Bgt was used to identify the first neuronal nAChRs, although this classification was initially controversial (*3*). Mammalian central nervous system [^{125}I]α-Bgt binding sites correspond to homomeric α7 nAChRs (*4*−*6*). However, it has become apparent that α-Bgt also interacts with α8* (*7*) and α9α10 nAChRs (*8*) in addition to the α1 muscle-type and α7 subtypes mentioned above, all at approximately nanomolar affinity. Further, the exceptionally slow binding kinetics of [^{125}I]α-Bgt to α7 nAChRs make equilibrium binding studies impractical. The norditerpenoid alkaloid methyllycaconitine (MLA) isolated from *Delphinium* sp. is a competitive antagonist for α7 nAChRs, with approximately nanomolar affinity and more useful kinetic properties (*9*). Unfortunately, MLA also interacts with α6* nAChRs with relatively high affinity (*10*−*12*). α9α10 nAChRs are difficult to express heteromerically, but chimeric subunits (containing the N-terminal ligand binding domain of each subunit, fused in each case to the C-terminal of a 5-HT$_{3A}$ subunit) express well and also bind [^{3}H]MLA with nanomolar affinity (*13*). Despite nearly 3 decades of work, no compound truly selective for α7 nAChR has been found.

Cone snails (genus *Conus*) produce a vast array of peptide toxins that target ion channels, including nAChRs, with exceptional selectivity. The conopeptide family that targets nAChRs (α-conotoxins, usually abbreviated to α-Ctxs) consists of small (13−19 residue) peptides, internally cross-linked by a pair of disulfide bridges. α-Conotoxins target narrow ranges of nAChR subtypes, and sometimes individual subtypes, with an unprecedented degree of specificity (*14*, *15*). They therefore offer an abundant source of leads for investigators attempting to discover novel, highly selective nAChR-targeted compounds.

Since α-Ctxs are short peptides, they and their analogues may be synthesized de novo by standard peptide synthesis

† This work was supported by NIH Grants DA12242 (to P.W. and J.M.M.), MH 53631 (to J.M.M.), and GM 48677 (to B.M.O. and D.Y.).

* Corresponding author. Tel: (303) 492-8844. Fax: (303) 492-8063. E-mail: wpaul@colorado.edu

‡ University of Colorado.

§ Department of Biology, University of Utah.

|| The Salk Institute.

⊥ Department of Psychiatry, University of Utah.

[1] Abbreviations: α-Bgt, α-bungarotoxin; α-Ctx, α-conotoxin; nAChRs, nicotinic acetylcholine receptors.

10.1021/bi7004202 CCC: $37.00
Published on Web 05/12/2007

techniques. In this study, a pair of peptides (corresponding to differentially processed potential products of a single clone from *Conus arenatus*) were synthesized. Both peptides, designated α-CtxArIA and α-CtxArIB, showed low nanomolar affinity for α7 homomeric nAChRs heterologously expressed in *Xenopus* oocytes but also had substantial affinity for the α3β2 subtype. α-CtxArIB had the highest selectivity (33-fold, compared to 3-fold for α-CtxArIA) for α7 over α3β2 nAChRs. By reference to previous structure−activity studies with α-CtxPIA (*16*) and α-CtxMII (*17*), a series of directed substitutions were made in α-CtxArIB, resulting in analogues with reduced α3β2 affinity while preserving potency for α7 nAChRs. When assessed in functional assays using heterologously expressed nAChR subtypes, the most selective analogue, α-CtxArIB[V11L,V16D], was 800- to >10000-fold more potent against α7 than all other nAChR subtypes, with minute-scale on-rate and off-rate kinetics. When tested against native nAChR subtypes in displacement binding assays, it also showed low nanomolar affinity for α7 and poor to no affinity for non-α7 nAChR subtypes.

EXPERIMENTAL PROCEDURES

Identification and Sequencing of a Genomic Clone. Genomic DNA was prepared from 50 mg of *C. arenatus* hepatopancreas using the Gentra PUREGENE DNA isolation kit (Gentra Systems, Minneapolis, MN) according to the manufacturer's standard protocol. Isolated DNA was used as a template for polymerase chain reaction (PCR) with oligonucleotides corresponding to the conserved intron and 3′ UTR sequences of α-conotoxin pre-propeptides. The resulting PCR products were purified using the High Pure PCR product purification kit (Roche Diagnostics, Indianapolis, IN) following the manufacturer's suggested protocol. The eluted DNA fragments were annealed to pAMP1 vector and the resulting products transformed into competent DH5α cells, using the CloneAmp pAMP system for rapid cloning of amplification Products (Life Technologies/Gibco BRL, Grand Island, NY). The nucleic acid sequences of the resulting α toxin-encoding clones were subsequently determined.

Chemical Synthesis. Method 1. Peptides (0.45 mmol/g) were synthesized using Fmoc chemistry with a Arg(pentamethyldibenzofuran-5-sulfonyl)-Wang resin (Novabiochem no. 04-12-20-44, San Diego, CA) and standard side protection, except on cysteine residues. Fmoc removal was accomplished with 20% piperidine in *N*-methylpyrrolidone. Cys residues were protected in pairs. The first and third Cys residues were protected with *S*-trityl groups, while *S*-acetamidomethyl protection was used for the second and fourth Cys residues. The completed peptides were cleaved from the resin with trifluoroactic acid−H_2O−ethanedithiol−phenol−thioanisole (90/5/2.5/7.5/5) by volume, which also removed the *S*-trityl groups from the first and third Cys. The peptide was precipitated, and a two-step oxidation protocol was used to selectively fold the peptides as described previously (*17*).

Chemical Synthesis. Method 2. In addition, α-CtxArIB-[V11L,V16D] was also synthesized manually on a Boc-Arg-(Tos)-CM resin (0.31 mequiv of Arg/g). The following side chain protected Boc-amino acids were used: Cys(Mob), Asn-(Xan), Arg(Tos), Ser(Bzl), His(Dnp), Asp(Chx), and Glu-(Chx). Most amino acid couplings were achieved in 40 min using diisopropylcarbodiimide in *N*-methylpyrrolidone in the presence of HOBt and monitored by the qualitative ninhydrin test of Kaiser and the tetrachloro-1,4-benzoquinone−acetaldehyde reagent for proline. A second coupling using 4 equiv of Boc-Asn(Xan) (based on the original substitution of the resin) preactivated in NMP with 3.9 equiv of HBTU, 8 equiv of HOBT, and 12 equiv of DIPEA followed prolines at positions 7 and 14. Boc removal was achieved with trifluoroacetic acid (60% in CH_2Cl_2, 1% *m*-cresol) for 10 min. After deblocking, the resin was washed with methanol followed by successive washes with triethylamine (10% in CH_2Cl_2), methanol, triethylamine (10% in CH_2Cl_2), methanol, and CH_2Cl_2. Before the last Boc-group deblocking, the Dnp protecting group was removed using thiophenol in NMP (15 equiv, 2 h). The completed peptide was then cleaved from the peptido-resin by HF containing anisole (10% v/v) and methyl sulfide (5% v/v) for 60 min at 0 °C. The deprotected and cleaved peptide was precipitated in diethyl ether with 1% (v/v) mercaptoethanol and separated from the spent resin by filtration after dissolution in water containing 0.1% trifluoroacetic acid (v/v). The major and desired component was isolated using preparative reverse-phase HPLC and an acetonitrile (solvent B) gradient of 0.1% trifluoroacetic acid−water (gradient 0−100% B/100 min). The fully reduced peptide eluted at ca. 26% B (16.5% acetonitrile). The fractions containing the desired peptide (250 mL) were combined and degassed with argon for 5 min. A buffer solution (2000 mL) made of distilled water, 15.4 g (0.2 mol) of ammonium acetate, 100 mg of EDTA (0.27 mmol), 500 mg of cysteine hydrochloride (3.2 mmol), and 500 mg of cystine (2.1 mmol) was also degassed using argon and added to the reduced peptide solution (250 mL); the pH (ca. 6.4) was immediately adjusted to 8.2 with freshly made ammonium carbonate solution (10%). The clear solution was stirred under argon for 20 h at room temperature. The folding was followed by HPLC.

After the folding was completed, the reaction mixture was acidified with trifluoroacetic acid, and the acetonitrile was removed under vacuum and then loaded to a preparative HPLC cartridge (5 cm × 30 cm) packed in the laboratory with reversed-phase 300 Å Vydac C_{18} silica (15−20 μm particle size). CtxArIB[V11L,V16D] eluted at 26% B with a flow rate of 100 mL/min using a linear gradient of 1% B/min increase, starting from 0% B (eluent A = 0.1% trifluoroacetic acid, pH 2.25; eluent B = 0.1% trifluoroacetic acid and 60% CH_3CN). Analytical HPLC screening of the purified fractions was performed on a Vydac C_{18} column (0.46 × 25 cm, 5 μm particle size, 300 Å pore size) and a 0.1% trifluoroacetic acid solvent system in isocratic condition.

Characterization of α-CtxArIB[V11L,V16D]. HPLC characterization of the fully oxidized peptide was performed under conditions of buffer A = TEAP (pH 2.5) and buffer B = 60% CH3CN/40% A with a gradient slope of 1% B/min, at flow rate of 0.2 mL/min on a Vydac C_{18} column (0.21 × 15 cm, 5 μm particle size, 300 Å pore size). UV absorbance was monitored at 214 nm.

Capillary zone electrophoresis (CZE) was done using a Beckman P/ACE System 2050 controlled by an IBM Personal System/2 Model 50Z and using a ChromJet integrator. Conditions: field strength of 15 kV at 30 °C; mobile phase, 100 mM sodium phosphate (85:15 H_2O:CH_3CN), pH

2.50, on a Supelco P175 capillary (363 μm o.d. × 75 μm i.d. × 50 cm length) with detection at 214 nm.

Mass spectra (MALDI-MS) were measured on an ABI-Perseptive DE-STR instrument. The instrument employs a nitrogen laser (337 nm) at a repetition rate of 20 Hz. The applied accelerating voltage was 20 kV. Spectra were recorded in delayed extraction mode (300 ns delay). The spectra were recorded in the positive reflector mode. Spectra were sums of 100 laser shots. Matrix α-cyano-4-hydroxy-cinnamic acid was prepared as saturated solutions in 0.3% trifluoroacetic acid in 50% acetonitrile.

Testing of Ligands on Recombinant nAChRs in Xenopus laevis Oocytes. The oocyte recording chamber was fabricated from Sylgard and was 30 μL in volume. Oocytes were gravity-perfused with ND96 (96.0 mM NaCl, 2.0 mM KCl, 1.8 mM $CaCl_2$, 1.0 mM $MgCl_2$, 5 mM HEPES, pH 7.1−7.5) containing 1 μM atropine (ND96A) with or without toxin at a rate of ∼1 mL/min. All solutions also contained 0.1 mg/mL bovine serum albumin (BSA) to reduce nonspecific adsorption of peptide. The perfusion medium could be switched to one containing peptide or ACh by use of a series of three-way solenoid valves (model 161T031; Neptune Research, Northboro, MA). All recordings were made at room temperature (∼22 °C). Oocytes were harvested and injected with cRNA encoding rat neuronal and human muscle nAChR subunits as described previously with the α6/α3 chimera Ala278 corrected to Val (*18*). ACh-gated currents were obtained with a two-electrode voltage-clamp amplifier as previously described (*18*).

To apply a pulse of ACh to the oocyte, the perfusion fluid was switched to one containing ACh for 1 s. This was automatically done at intervals of 1−2 min. The shortest time interval was chosen such that reproducible control responses were obtained with no observable desensitization. This time interval depended on the nAChR subtype being tested. The concentration of ACh was 200 μM for α7, 10 μM for α1$\beta\gamma\delta$ and α9α10, and 100 μM for all other subtypes. The ACh was diluted in ND96A for tests of all nAChR subtypes except α7 and α7α10, in which case the diluent was ND96. For control responses, the ACh pulse was preceded by perfusion with ND96 (for α7 and α9α10) or ND96A (all others). No atropine was used with oocytes expressing α7 and α9α10, because it has been demonstrated to be an antagonist of α7-like receptors (*19*). For test responses, toxin was bath applied for 5 min prior to subsequent exposure to ACh. For kinetic experiments and toxin concentrations less than 1 μM, the perfusion medium was switched to one containing peptide or ACh by use of a distributor valve (SmartValve; Cavro Scientific Instruments, Sunnyvale, CA) and a series of three-way solenoids. When the perfusion solution was switched to one containing toxin, the same interval of ACh pulses was maintained. Toxin was continuously perfused until responses reached a steady state. To conserve toxin in tests at high toxin concentrations (1 μM or greater), the oocyte was exposed to peptide in a static bath for 5 min prior to initiation of ACh pulses. All ACh pulses contained no toxin, for it was assumed that little, if any, bound toxin would have washed away in the brief time (<2 s) it takes for the responses to peak. The average peak amplitudes of three control responses just preceding exposure to toxin were used to normalize the amplitude of each test response to obtain "% response" or "% block." Occasionally during off-rate determinations, responses would recover to levels above 100% of control responses. This "baseline drift" was corrected for by curve fitting, see next. Each data point of a dose−response curve represents the average value ± SEM of measurements from at least three oocytes.

Kinetic Modeling. When a receptor has multiple binding sites for a toxin, then the relationship between the level of functional block produced by the toxin and the level of toxin occupancy of sites on the receptor can be nonlinear as described by ref *20* for a receptor with N independent (i.e., noninteracting) toxin-binding sites. This model was used to analyze the present study's results. Data fits were performed with Prism software (GraphPad Software, San Diego, CA) or SigmaPlot V9.0.1 (Systat Software Inc., Point Richmond, CA), which gave identical results.

For off-rate kinetics, data were fit to

$$A_t = (mt + c) + 100\%(1 - e^{-k_{off}t})^N \quad (1)$$

where A_t is activity at time t, m is the slope of baseline drift, c is the residual response at $t = 0$ (the instant before toxin washout is commenced), k_{off} is the off-rate constant, and N is the number of equivalent toxin-binding sites on the receptor, where occupation of any one site is sufficient to functionally inactivate the receptor. The time course of the recovery from block (eq 1) following washout of a saturating concentration of toxin has a very distinct lag when $N > 1$ and can provide an estimate of the value of N. Experimentally derived values of N were consistently close to $N = 5$ for α7 nAChRs (see Results section), which fits with the concept of a homopentamer of α7 subunits. For this reason, individual experiments were fit using $N = 5$.

For on-rate kinetics, data were fit to the equation:

$$A_t = 100\%\left\{1 - \frac{1 - e^{-k_{obs}t}}{1 + K_d/[T]}\right\}^N \quad (2)$$

where A_t is activity at time t following toxin exposure, k_{obs} is the observed decay constant, [T] is the concentration of toxin applied at $t = 0$, and N is the number of equivalent toxin-binding sites. K_d and k_{obs} may be defined in terms of true on and off rates (k_{on} and k_{off}, respectively):

$$K_d = k_{off}/k_{on} \quad (3)$$

$$k_{obs} = k_{on}[T] + k_{off} \quad (4)$$

By doing so, and substituting in the experimentally defined value of [T], together with the experimentally derived values of k_{off} and N, k_{on} may be determined.

When $t = \infty$, i.e., when the reaction is at equilibrium, eq 2 reduces to

$$FA(\infty) = \left\{1 - \frac{1}{1 + K_d/[T]}\right\}^N \quad (2b)$$

This equation was used to calculate K_d values for peptide/receptor equilibrium binding (Figures 2 and 3).

When $FA(\infty) = 0.5$, by definition $[T] = IC_{50}$. Substituting these values into eq 2b yields

$$IC_{50}/K_d = 2^{1/N} - 1 \quad (2c)$$

Thus, for example, when $N = 5$, $K_d/IC_{50} = 6.725$. The derivations of eqs 1 and 2 are given in ref *20*.

α-CtxArIB[V11L,V16D] Binding Assays Using Native nAChR Subtypes. Mouse brain membranes were prepared from male mice (C57BL/6J, 60−120 days old). Mice were bred at the Institute for Behavioral Genetics and housed five per cage. The vivarium was maintained on a 12 h light/dark cycle, and mice were given free access to food and water. All procedures used in this study were approved by the Animal Care and Utilization Committee of the University of Colorado. Each mouse was sacrificed by cervical dislocation, and the brain was removed and placed on an ice-cold platform. Tissue was collected from the hippocampus, inferior colliculus, interpeduncular nucleus, medial habenula, olfactory bulbs, olfactory tubercles, superior colliculus, striatum, and thalamus. Individual regional samples were homogenized in ice-cold hypotonic buffer (mM: NaCl, 14.4; KCl, 0.2; $CaCl_2$, 0.2; $MgSO_4$, 0.1; HEPES 2; pH = 7.5) using a glass−Teflon tissue grinder (*21*). Particulate fractions were collected by centrifugation at 25000*g* (15 min, 4 °C; Eppendorf 5417 C centrifuge). The pellets were resuspended in fresh homogenization buffer, incubated on ice for 10 min, and then harvested by centrifugation as before. Each pellet was washed twice more by resuspension/centrifugation before storage (in pellet form under homogenization buffer) at −70 °C until used.

Frozen *Torpedo californica* electroplax tissue was obtained from Aquatic Research Consultants (San Pedro, CA). Tissue was thawed on ice and then homogenized (3 × 5 s at full speed) using a Polytron homogenizer (Brinkmann Instruments, Westbury, NY) in ice-cold isotonic binding buffer (mM: NaCl, 144; KCl, 2; $CaCl_2$, 2; $MgSO_4$, 1; HEPES 20; pH = 7.5) supplemented with bovine serum albumin [0.1% (w/v)] and protease inhibitors (5 mM EDTA, 5 mM EGTA, 1 mM phenylmethanesulfonyl fluoride, and 10 μg/mL each of aprotinin, leupeptin trifluoroacetate, and pepstatin A; protease inhibitor buffer) to minimize proteolysis. Membranes were collected by centrifugation (25000*g*, 30 min, 4 °C), and the resulting pellets were rehomogenized as before. The resulting membranes were washed twice more by resuspension in protease inhibitor buffer and centrifugation before storage (in pellet form under homogenization buffer) at −70 °C until used.

The selectivity of α-CtxArIB[V11L,V16D] was assessed by a panel of displacement binding assays using the membrane preparations described above. Affinity for α7 nAChRs was measured by displacement of [^{125}I]α-Bgt binding to hippocampal membranes. A slightly modified version of the 96-well format assay described by ref *10* was used. Incubations were performed at 22 °C for 4 h in 1.2 mL polypropylene tubes arranged in a 96-well format. Hippocampal membranes were incubated with 2 nM high specific activity [^{125}I]α-Bgt (2000 Ci mmol^{-1}; GE Healthcare, Piscataway, NJ) in a total volume of 30 μL of isotonic binding buffer supplemented with protease inhibitors. The ability of a range of α-CtxArIB[V11L,V16D] concentrations (0.3 nM−10 μM) to displace [^{125}I]α-Bgt binding was assessed. Nonspecific binding was defined using 10 μM α-cobratoxin. Following the initial incubation, 1 mL of isotonic binding buffer, supplemented with bovine serum albumin [0.1% (w/v)], was added to each tube, and the incubation was continued for a further 5 min at 22 °C. This dilution and further incubation step allows some of the nonspecific binding to dissociate but has no measurable effect on specific binding, increasing the signal to noise ratio of the binding assay. Binding reactions were terminated by filtration using a 96-place manifold (Inotech Biosystems, Lansing, MI). Particulate fractions were collected onto single layers of Inotech 0.75 μm retention glass fiber filters that had been soaked in 5% nonfat skim milk dissolved in isotonic binding buffer. Samples were washed six times, and all filtration and washing were conducted in a 4 °C cold room, using ice-cold buffer. Bound radioligand was quantified by γ counting at 83−85% efficiency, using a Packard Cobra counter (Perkin-Elmer Life and Analytical Sciences, Inc., Wellesley, MA). Inhibition of [^{125}I]α-Bgt binding to *Torpedo* membranes was used to measure the affinity of α-CtxArIB-[V11L,V16D] for muscle-type $\alpha1\beta1\gamma\delta$ nAChRs. Identical assay conditions were used as those described for [^{125}I]α-Bgt binding to hippocampal membranes.

α-CtxArIB[V11L,V16D] affinity for [^{125}I]α-CtxMII-binding nAChRs [$\alpha6\beta2$* subtype (*22*)] was assessed using pooled membranes from mouse olfactory tubercle, striatum, and superior colliculus. The conditions were the same as described in ref *10* and very similar to those described above for [^{125}I]α-Bgt binding, with the following modifications. [^{125}I]α-CtxMII (2200 Ci mmol^{-1}), synthesized as described (*23*), was used at 0.5 nM, initial incubations proceeded for 2 h, and incubations were continued for 4 min after the dilution step. Bound radioligand was quantitated by γ counting, as described above.

The interaction between α-CtxArIB[V11L,V16D] and $\alpha4\beta2$* nAChRs was probed using displacement of [^{3}H]-cytisine (5 nM, 21.2 Ci mmol^{-1}; NEN, Boston, MA) binding to mouse thalamic membrane preparations. Incubations were performed at 22 °C for 1 h in polystyrene 96-well plates. A total volume of 100 μL of isotonic binding buffer supplemented with protease inhibitors was used for incubations. α-CtxArIB[V11L,V16D] concentrations of 0.3 nM−10 μM were used, and blanks were defined using 100 μM (−)-nicotine tartrate. Binding reactions were terminated by filtration onto single layers of Inotech 0.75 μm retention glass fiber filters that were soaked in 0.5% polyethylenimine for [^{3}H]cytisine assays. Samples were washed as described for [^{125}I]α-Bgt binding. Following addition of 1 mL of Budget Solve scintillation fluid (Research Products International, Mount Prospect, IL) to each sample, bound radioligand was quantitated by liquid scintillation counting (at 45% efficiency), using a Packard 1600 TR liquid scintillation spectrometer.

Finally, the affinity of α-CtxArIB[V11L,V16D] for native $\beta4$* nAChRs was measured using inhibition of [^{125}I]-epibatidine (200 pM, 2200 Ci mmol^{-1}; NEN, Boston, MA) binding in the presence of the $\beta2$* nAChR-selective agonist A85380 (10 nM, unlabeled), as described in ref *24*. The inferior colliculus, interpeduncular nucleus, medial habenula, and olfactory bulbs contain relatively high proportions of $\beta4$* nAChRs when compared to other brain regions (*24*), so membranes from these regions were used in the present study. A total incubation volume of 30 μL of isotonic binding buffer supplemented with protease inhibitors was used, and incubations proceeded at 22 °C for 2 h in polystyrene 96-well plates. Nonspecific binding was again defined in the presence of 100 μM (−)-nicotine tartrate, and binding

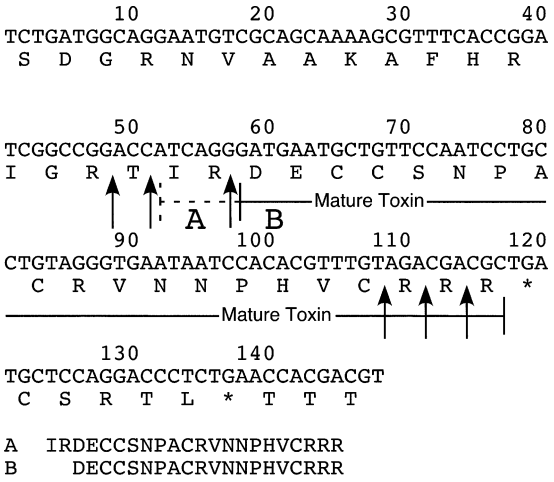

FIGURE 1: Pre-propeptide and toxin-coding region from *C. arenatus*. Possible proteolytic processing sites are indicated (arrows). Peptides α-CtxArIA and α-CtxArIB, derived from this clone, are shown.

reactions were terminated and washed as described for [^{3}H]-cytisine, above.

RESULTS

Cloning of an α-Conotoxin from C. arenatus. α-Conotoxins are processed from a larger precursor protein. A high degree of conservation among the introns of α-conotoxins from different *Conus* species as well as the 3′-untranslated regions of the mRNAs allows for a molecular approach to toxin discovery (*25*). The conserved features of the gene structure were employed to devise oligonucleotide primers for polymerase chain reaction amplification of the toxin-coding region. The cDNA clone from *C. arenatus* is shown in Figure 1.

Chemical Synthesis of α-Conotoxins Based on the C. arenatus Clone. Proteolytic cleavage of conotoxins from their precursor form generally occurs after a basic residue. The *arenatus* conotoxin clone showed multiple possible processing sites, particularly at the C-terminus. In addition, the N-terminal portion of the clone shows identity to α-conotoxin GID that begins with the sequence IRD (*26*). We therefore initially elected to synthesize two of the possible translation products, named respectively α-CtxArIA and α-CtxArIB (Figure 1). Solid-phase synthesis of the possible mature toxins, as well as all subsequent analogues, assumed that the disulfide bridging was the same as that of previously characterized α 4/7 α-conotoxins that were purified from venom, i.e., first Cys to third Cys and second Cys to fourth Cys. To accomplish this, Cys groups were orthogonally protected in pairs to direct the disulfide bond formation as described in Experimental Procedures. The masses of the synthetic peptides were confirmed in each instance with matrix-assisted laser desorption mass spectrometry.

Synthesis was routine in all cases except for the final analogue. In the case of α-CtxArIB[V11L,V16D], the first attempt at synthesis using method 1 (Experimental Procedures) resulted in a major product which, after cleavage from resin, was 18 Da less than the calculated mass. We suspected that the introduction of an Asp in position 16 had led to aspartimide formation as the result of a side reaction that can occur in Fmoc synthesis due to the strongly basic conditions during deprotection. This can be particularly

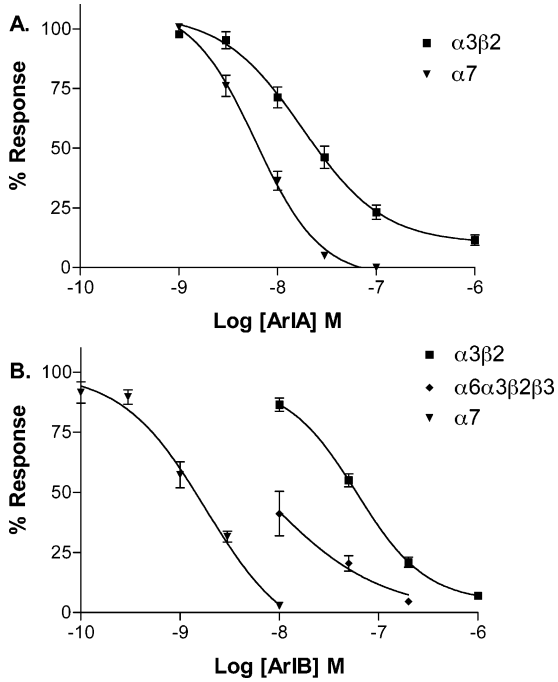

FIGURE 2: Effect of α-CtxArIA and α-CtxArIB on nAChRs. The peptides were tested on nAChRs expressed in *Xenopus* oocytes as described in Experimental Procedures. (A) ArIA blocks α7 and α3*β*2 nAChRs with IC_{50}s of 6.02 (4.51−8.02) nM and 18.0 (10.7−30.1) nM and Hill slopes of 1.3 ± 0.22 and 1.1 ± 0.27, respectively; n = 3−5. (B) α-CtxArIB blocks α7, α3*β*2, and α6/α3*β*2*β*3 nAChRs with IC_{50}s of 1.81 (0.922−3.54), 60.1 (43.4−83.2), and 6.45 (2.94−14.2) nM and Hill slopes of 1.0 ± 0.39, 1.2 ± 0.25, and 0.74 ± 0.17, respectively. n = 3−4; error bars, 95% confidence interval; ±, standard error of the mean.

problematic when Asp occurs near the COOH terminus since repeated exposure to base occurs during repetitive deprotection cycles (*27*). Consistent with this, reduction of deprotection time from 40 to 14 min resulted in the major cleavage product having the correct mass. In addition, use of Fmoc Asp(*O*-3-methylpentyl)-OH rather than Fmoc-Asp(*tert*-butyl)-OH further improved the yield of the correct vs −18 Da product. Finally (method 2, Experimental Procedures), α-CtxArIB[V11L,V16D] was also synthesized manually on a Boc-Arg(Tos)-CM resin using the Boc strategy and cleaved in HF to yield the fully deprotected reduced peptide. After an initial preparative RP-HPLC purification step using a 0.1% trifluoroacetic acid in water/acetonitrile gradient, the peptide was oxidized/folded using the cysteine/cystine redox system. Under these conditions, the peptide folded in 20 h to give a single isomer. Oxidized peptide was purified using preparative RP-HPLC and mass confirmed with matrix-assisted laser desorption mass spectrometry. The peptide (synthetic method 2) coeluted with peptide prepared by directed disulfide folding (synthetic method 1) using both RP-HPLC and capillary zone electrophoresis with conditions described in Experimental Procedures. The overall yield of highly purified material was 17%.

Activity and Design of Peptide Analogues. The synthetic ligands α-CtxArIA and α-CtxArIB were applied to nAChRs heterologously expressed in *Xenopus* oocytes to test their abililty to block the response to ACh. Both peptides potently blocked the α7 and α3*β*2 subtypes of nAChRs, with lower IC_{50}s on α7. α-CtxArIB was more potent than α-CtxArIA on α7 and also showed a larger difference in IC_{50} between

Table 1: Selectivity of α-Conotoxins and Analogues

peptide	sequence	IC_{50} (nM) for block of *Xenopus* oocyte-expressed nAChRs				
		α7	α3β2	α6α3β2β3	ratio α3β2/α7[a]	ratio α6α3β2β3/α7[b]
ArIA	IRDECCSNPACRVNNOHVCRRR[e]	6.02	18.0	ND	2.99	
ArIB	DECCSNPACRVNNPHVCRRR[e]	1.81	60.1	6.45	33.2	3.56
ArIB[N6R,A8P]	DECCSRPPCRVNNPHVCRRR[e]	15.9	24.4	ND	1.53	
ArIB[V11L]	DECCSNPACRLNNPHVCRRR[e]	0.539	38.8	ND	72	
ArIB[V11L,V16A]	DECCSNPACRLNNPHACRRR[e]	0.356	74.5	120	209	337
ArIB[V11L,V16D]	DECCSNPACRLNNPHDCRRR[e]	1.09	>10000	828[g]	>10000	760[g]
PnIA[c]	GCCSLPPCAANNPDYC[f]	252	9.56	ND	0.0379	
PnIA[A10L]	GCCSLPPCALNNPDYC[f]	12.6	99.3	ND	7.9	
MII[d]	GCCSNPVCHLEHSNLC[f]	130	2.2	0.39	0.017	0.00300
MII[L15A][d]	GCCSNPVCHLEHSNAC[f]	ND	34.1	0.917		

[a] (α3β2 IC_{50})/(α7 IC_{50}). [b] (α6/α3β2β3 IC_{50})/(α7 IC_{50}). [c] Data from ref *1*. [d] Data from ref *2*; O, 4-hydroxyproline. [e] Free carboxy. [f] Amidated C-terminus; ND, not determined. [g] Maximum block for α6α3β2β3 was 39%.

α7 and α3β2 nAChRs (Figure 2 and Table 1). We therefore selected α-CtxArIB for further study. α-CtxArIB was also found to have significant affinity for α6/α3β2β3 nAChRs, where α6/α3 is a chimera that contains the extracellular binding portion of the α6 subunit joined to the transmembrane and intracellular portion of α3 (*19*).

Since the peptide had high affinity for three subtypes of nAChRs, we next sought to make an analogue that would selectively act on the α7 nAChR. α-CtxArIB is a two-bridge peptide with four residues in the first loop and seven in the second and therefore belongs to the α 4/7 class of α-conotoxins. Solution NMR and X-ray crystallography analyses of other α 4/7 conotoxins show a high degree of conservation of the peptide backbone conformation among members of this class. This indicates that selectivity profiles of the various α 4/7 peptides are likely due to difference in amino acid side chains rather than the conformation of the peptide per se (*28*). Initial experiments with an analogue in which two amino acids in the first loop were substituted were not promising. Substitutions N6A,A8P in α-CtxArIB decreased affinity at α7 and increased affinity for α3β2 (Figure 3A). We next tried substitutions based on structural comparisons of α-CtxArIB with two other peptides, α-CtxPnIA and α-CtxMII. α-CtxPnIA nonselectively blocks α3β2 nAChRs with a lower IC_{50} compared to that observed for α7 nAChRs. Nevertheless, structure−activity studies of α-PnIA indicate that an A10L substitution shifts affinity for α7 and α3β2 in favor of α7 nAChRs (Table 1) (*29*). We therefore assessed whether a V11L substitution present in the homologous position in the α-CtxArIB peptide would selectively reduce activity at α3β2 nAChRs. Indeed, the V11L substitution increased affinity for α7 relative to that of α3β2. α-CtxMII is a conotoxin that potently blocks α3β2 and α6-containing nAChRs. Structure−activity studies of α-CtxMII indicate that an L15A substitution weakens activity at α3β2 nAChRs (*29*). We therefore tried a similar substitution, namely, V16A, in the α-CtxArIB peptide. Activity at α3β2 was weakened without negative effect on α7. Thus, for the α-CtxArIB analogue, residue change at position 16 selectively modified receptor subtype affinity. Since position 16 was permissive with respect to activity at α7, we sought to further weaken activity at α3β2 by a V16D substitution. Asp differs from Ala in that the former has a negatively charged carboxyl group instead of a hydrogen on the terminal carbon of the side chain. This substitution had a relatively modest negative effect on α7 activity compared to the more substantially negative effect on α3β2 and α6/α3β2β3 activity. The final analogue was >10000-fold selective for α7 vs α3β2, compared to 3- and 30-fold for the parent peptides α-CtxArIA and α-CtxArIB, respectively (Figure 3 and Table 1).

Selectivity and Kinetics of Block by α-CtxArIB[V11L,V16D]. α-CtxArIB[V11L,V16D] was tested on additional nAChR subtypes. The peptide had an IC_{50} > 20 μM for α1β1γδ, α2β2, α2β4, α3β2, α3β4, α4β2, α4β4, α6/α3β2β3, α6/α3β4, and α9α10 nAChRs expressed in *Xenopus* oocytes (data not shown). Kinetics of block were assessed on α7, the nAChR subtype against which the peptide was most potent. Functional block by both the α-CtxArIB parent peptide and the α-ArIB[V11L,V16D] analogue was slowly reversible. The time course of recovery from block at high toxin concentrations invariably had a distinctive lag (Figure 4), and the results (given in detail in the legend to Figure 4) of curve fitting of the data to eq 1 in Experimental Procedures are consistent with five binding sites for both α-CtxArIB and α-CtxArIB[V11L,V16D] on the α7 receptor, where occupation of any one site is sufficient to block function. Concentration response data shown in Figures 2 and 3 were also used to calculate K_ds for α7 nAChRs using eq 2b and utilizing $N = 5$ for binding sites. These K_ds were 10.3 ± 0.95 nM for ArIB and 12.6 ± 2.1 nM for ArIB[V11L,V16D], in good agreement with those obtained from kinetic analysis (Figure 4).

Activity of α-CtxArIB[V11L,V16D] on native nAChRs was assessed in competition binding studies using mouse brain and *Torpedo* electroplax homogenates (Figure 5). The outcome was consistent with the selectivity profile determined in functional studies with cloned rat nAChRs. α-CtxArIB[V11L,V16D] displaced [^{125}I]α-Bgt binding in mouse hippocampal membranes [corresponding to α7* nAChRs (*4*, *5*)] with a K_i (or K_d of Ctx) of 7.04 nM. This agrees well with the K_d determined through kinetic analysis of α-CtxArIB[V11L,V16D] functional block (8.26 nM; see legend to Figure 4 for details). Further, if there are five identical independent binding sites per pentameric α7 nAChR, and only one site per receptor needs to be occupied to block receptor function, this would correspond to a predicted functional IC_{50} of 1.05 nM (see eq 2c in Experimental Procedures) closely matching the value of 1.09 nM observed in oocyte-expression experiments (Figure 3D). α-CtxArIB[V11L,V16D] made by the two different synthetic procedures produced indistinguishable results. α-CtxArIB-[V11L,V16D] concentrations as high as 10 μM had no effect on binding to α4β2* nAChRs (measured with [^{3}H]cytisine binding to mouse thalamic membranes), α1β1γδ muscle-

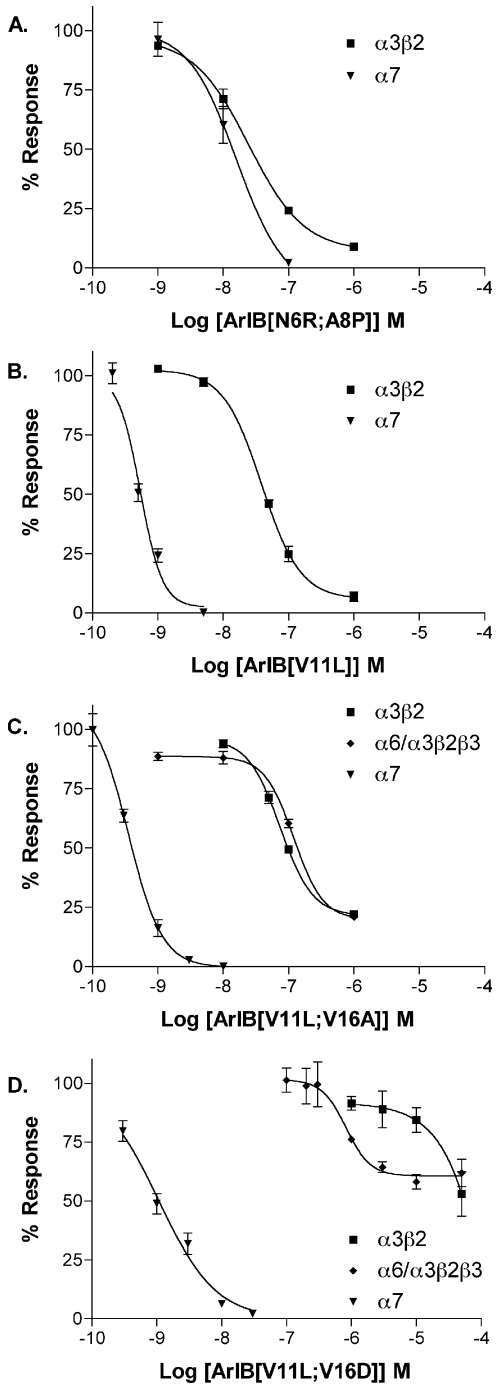

FIGURE 3: Effect of α-CtxArIB analogues on nAChRs. The peptides were tested on nAChRs expressed in *Xenopus* oocytes as described in Experimental Procedures. (A) α-CtxArIB[N6R,A8P] blocks α7 and α3*β*2 nAChRs with IC_{50}s of 13.0 (8.14−20.8) and 24.4 (16.6−35.9) nM and Hill slopes of 1.9 ± 1.3 and 1.0 ± 0.25, respectively. (B) α-CtxArIB[V11l] blocks α7 and α3*β*2 nAChRs with IC_{50}s of 0.538 (0.458−0.634) and 38.8 (26.4−57.0) nM and Hill slopes of 2.6 ± 0.45 and 1.5 ± 0.34, respectively. (C) α-CtxArIB[V11L,-V16A] blocks α7, α3*β*2, and α6/α3*β*2*β*3 nAChRs with IC_{50}s of 0.356 (0.286−0.443), 74.5 (65.0−85.3), and 120 (64.1−226) nM and Hill slopes of 1.7 ± 0.25, 1.8 ± 0.25, and 1.2 ± 0.24, respectively. (D) α-CtxArIB[V11L,V16D] blocks α7, α3*β*2, and α6/α3*β*2*β*3 nAChRs with IC_{50}s of 1.09 (0.878−1.34), >10000, and 828 (435−1570) nM, respectively. The maximum block for α6/α3*β*2*β*3 was 39.3%. The Hill slope for α7 was 1.0 ± 0.10. n = 4−9; error bars, 95% confidence interval; ±, standard error of the mean; data were plotted using eq 3.

type nAChRs (measured with [^{125}I]α-Bgt binding to *Torpedo californica* membranes), or *β*4* nAChRs [determined using A85380-resistant [^{125}I]epibatidine binding to each of mouse inferior colliculus, interpeduncular nucleus, medial habenula, or olfactory bulb membranes (*30*)]. The highest α-CtxArIB-[V11L,V16D] concentration used (10 μM) slightly reduced [^{125}I]α-CtxMII binding to α6*β*2* nAChRs [in pooled olfactory tubercle, striatal, and superior colliculus membranes (*10*)]. Where inhibition was seen, data were fit to a single-site logistic inhibition curve. The resulting IC_{50} values were converted to K_i values using the Cheng−Prusoff equation.

DISCUSSION

In this study we report the cloning and synthesis of a novel α-conotoxin from *C. arenatus.* Analysis of synthetic peptides based on the *C. arenatus* clone indicated potent activity at three nAChRs subtypes: α7, α6*β*2, and α6/α3*β*2*β*3. In an attempt to devise peptides with single subtype selectivity, we utilized, in part, structure−activity data for peptides that act on α3*β*2 nAChRs. α-CtxPnIA is from the mollusk-eating *Conus pennaceus*. α-CtxMII is from the fish-eating *Conus magus*. In contrast, *C. arenatus*, a snail that ranges from East Africa to the Marshall Islands, feeds on polychaete worms. Differing subtype selectivity of conotoxins from these different *Conus* species presumably is at least partly due to venom directed at prey from different phyla. Nevertheless, the present study suggests that information from structure−activity relationships of peptides from one distantly related cone species may be applicable to that of another. In this instance, the resulting α-CtxArIB[V11L,V16D] is the most selective α7 nAChR subtype ligand described to date.

Application of this probe provided significant insights into both its mechanism of action at α7 nAChRs and the structure of these receptors. Recovery-of-function analysis indicated that both unmodified α-CtxArIB and α-CtxArIB[V11L,-V16D] interact with five sites per receptor. Further, only one site out of five per receptor needs to be occupied for function to be blocked. This is consistent with the structure of α-conotoxin bound to the acetylcholine binding protein (*32*). Our results therefore support the application of modeling of the α7 nAChR based on the crystal structure of the acetylcholine binding protein.

Conotoxins ArIA and ArIB may or may not correspond exactly to naturally occurring conotoxins. For example, either or both putative proteolytic cleavage sites may be used by *C. arenatus*. It is also possible that the native toxin may have additional posttranslational modifications [for example, the C-termini of many native α-Ctxs are posttranslationally amidated (*51*)]. We did not try to identify a native peptide or peptides in *C. arenatus* venom that is/are derived from the ArIA/B cloned sequence. While very interesting, this would require a great deal of extra work, and our focus was on developing an α7-selective ligand with inspiration from, but not definitive knowledge of, the native peptide. This focus also informed our decision to proceed with peptides containing free C-termini: the original, unamidated ArIA/B peptides had considerable affinity at α7 nAChRs, and we retained this feature throughout our attempts to make more α7-selective derivatives.

Despite the caveats above, it is highly likely that the artificial peptide will have the same tertiary structure as other α 4/7 conotoxins since it has the conserved cystine and proline framework that is characteristic of this peptide class.

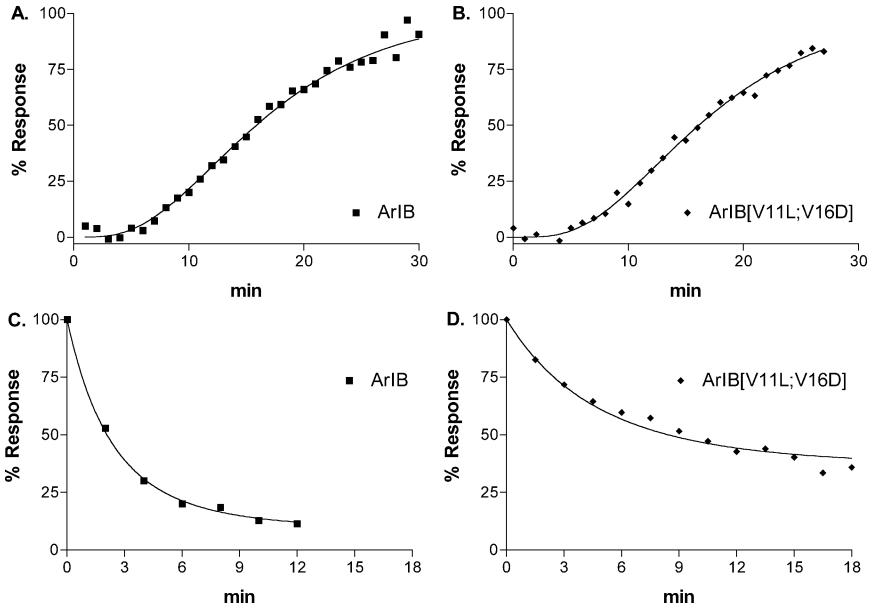

FIGURE 4: Kinetics of block by α-CtxArIB and α-CtxArIB[V11L,V16D]. Recovery from block by α-CtxArIB (A) and α-CtxArIB[V11L,-V16D] (B) was measured. Individual experiments are shown with baseline drift subtracted, but $n = 5$ for α-CtxArIB and $n = 6$ for α-CtxArIB-[V11L,V16D]. Mean k_{off} for α-CtxArIB dissociation was 0.125 ± 0.008 min^{-1} with 4.98 ± 0.53 binding sites predicted. The values calculated for α-CtxArIB[V11L,V16D] dissociation were very similar: average k_{off} was 0.122 ± 0.004 min^{-1} with 4.61 ± 0.15 sites predicted. When the data were re-fit, constraining the number of sites to five, average k_{off} values were calculated as 0.125 ± 0.008 and 0.128 ± 0.003 min^{-1} for α-CtxArIB and α-CtxArIB[V11L,V16D], respectively. Onset of block by α-CtxArIB (C) and α-CtxArIB[V11L,V16D] (D) was also measured. The peptides were perfused at concentrations of 3 and 1 nM, respectively, onto *Xenopus* oocytes expressing α7 nAChRs as described in Experimental Procedures. The response to a 1 s pulse of ACh was measured every 1 min. A single experiment is shown. Again, the experiment was repeated (α-CtxArIB, $n = 4$; α-CtxArIB[V11L,V16D], $n = 6$) on different oocytes. As detailed in Experimental Procedures, fixing the known parameters allows k_{on} to be calculated. Assuming five sites, the average k_{on} for toxin block was 0.0287 ± 0.0011 min^{-1} nM^{-1} for α-CtxArIB and 0.0155 ± 0.0031 min^{-1} nM^{-1} for α-CtxArIB[V11L,V16D]. Since $K_d = k_{off}/k_{on}$, the calculated association and dissociation rates can be used to determine K_d for each peptide, giving $K_d = 4.36$ nM for α-CtxArIB and 8.26 nM for α-CtxArIB[V11L,V16D].

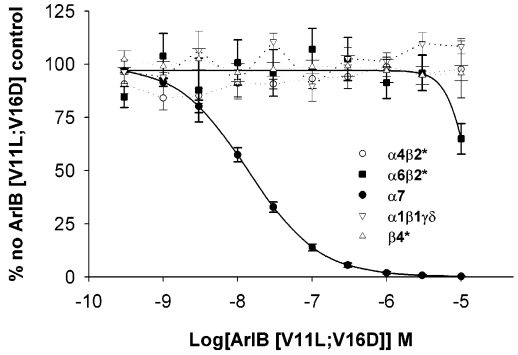

FIGURE 5: Displacement binding at native nAChR subtypes by α-CtxArIB[V11L,V16D]. The ability of α-CtxArIB[V11L,V16D] to displace nicotinic binding to native nAChR subtypes was measured as described in Experimental Procedures. α-CtxArIB-[V11L,V16D] inhibited [^{125}I]α-Bgt binding to α7 nAChRs in mouse hippocampal membranes with a k_i of 7.04 (5.16, 8.92) nM. At the other subtypes tested, $k_i > 10$ μM. Error bars show 95% confidence interval. For β4* nAChRs, only data collected from medial habenula membranes are shown, for clarity, although a similar lack of displacement was seen in the other regions studied. Points represent the mean ± standard error of the mean for three to five individual determinations.

Indeed, since multiple native α 4/7 conotoxins adopt essentially identical folds, it seems that their nAChR selectivity must be dictated by differences in side chain residues, rather than by differences in peptide conformation (*28*).

Because nonbackbone amino acids can be substituted without inducing major structural alterations, modified α-conotoxins can be synthesized to generate ligands with useful novel properties. Two examples using the well-characterized peptide α-CtxMII illustrate the utility of this approach. When first discovered, α-CtxMII was shown to selectively block heterologously expressed α3β2 subtype nAChRs (*34*). Subsequently, α-CtxMII was modified by addition of a non-native N-terminal tyrosine and radioiodination, producing [^{125}I]α-CtxMII, a radiolabel used to target native neuronal nAChRs. When it became clear that α-CtxMII had high affinity for both α3β2* and α6β2* nAChRs (*35*), a systematic mutational approach was taken to generate α6β2* selective (*17*). In the present study, a more directed approach was taken to lessen α-CtxArIB's affinity for α3β2 nAChRs, while preserving or enhancing affinity at α7 nAChRs. Lessons from structure−activity studies in α-Ctx-PnIA (*29*) and α-CtxMII (*17*) guided substitutions at the 10, 11, and 16 positions of α-CtxArIB, eventually producing a modified toxin (α-CtxArIB[V11L,V16D]) with similar-to-unmodified affinity for α7 nAChRs but with a much increased α3β2:α7 selectivity ratio (>10000-fold vs 33-fold).

Interestingly, in both the present study and in ref *17*, amino acid substitutions produced increased selectivity by reducing 'unwanted' affinity at α3β2 nAChRs rather than enhancing affinity at the subtype of interest. This may indicate that it is easier to considerably weaken nAChR/α-Ctx interactions than it is to find ways to substantially increase them where affinity is already high. This may not be surprising since α-conotoxins have been, and continue to be, naturally selected on the basis of their nAChR activity. In any case it seems that an approach of finding native sequences with high affinity for nAChR subtypes of interest, followed by refinement to remove significant affinities at other nAChR

Table 2: Activity of MLA on α7 nAChRs

assay	species	IC_{50} (nM)	k_i (nM)	ref
inhibition of [^{125}I]α-Bgt binding to hippocampal membranes	rat		4.3	*37*
block of ACh-induced whole cell currents in fetal hippocampal neurons	rat	0.20		*37*
decrease in frequency of single channel openings in fetal hippocampal neurons	chick	~0.001		*37*
inhibition of [^{125}I]α-Bgt binding to brain	chick		5.4	*50*

subtypes, may be generally applicable. As more structure−activity information becomes available, this directed substitution approach should become more powerful.

For example, another 4/7 conotoxin, α-CtxPeIA (*36*), interacts with 260-fold greater affinity at α9α10 compared to α7 nAChRs, the opposite selectivity to α-CtxArIB and its derivatives. α-CtxPeIA also has substantial affinity for α3β2 nAChRs, similar to its sister 4/7 toxins α-CtxArIB and α-CtxMII. These facts suggest two possibilities. First, it may be possible to generate a highly selective α9α10-directed peptide using a similar directed substitution approach to that described in this study (by selectively reducing α-CtxPeIA's affinity for α3β2 nAChRs). Second, it seems that α-conotoxins with the 4/7 fold may be particularly well suited to interacting with mammalian α3β2 nAChRs, perhaps because their intended target nAChR subtype(s) share(s) features with this subtype.

α7 nAChRs are often expressed alongside other subtypes, including those with substantial affinity for MLA and α-Bgt (which have commonly been used to identify α7 nAChRs). In the central nervous system, MLA-sensitive α6β2* nAChRs are concentrated in the dopaminergic projections of the substantia nigra and ventral tegmental area and the optic tract (*22*). These regions also contain α7 nAChRs, complicating efforts to identify α7 nAChRs specifically. MLA also has some practical disadvantages as a pharmacological tool. Several studies have reported widely disparate MLA affinities for α7 nAChRs, particularly when comparing its ability to functionally block receptors to its potency in competitive radioligand binding assays (Table 2). Further, difficulties in reliably establishing MLA's potency as an antagonist of α7 function, even in a single study, have been described (*37*, *38*). By comparison, as described in this study, α-CtxArIB-[V11L,V16D] reliably showed similar affinities in both functional and ligand binding assays. In the periphery, α7 nAChR gene and/or protein expression has been shown to overlap with that of the α-Bgt- and MLA-sensitive α9α10 subtype in cochlea (*39*), dorsal root ganglion (*40*), keratinocytes (*41*), and lymphocytes (*42*). Further, injured muscle coexpresses muscle type (α1*) and α7 nAChR subtypes (*43*), both of which bind α-Bgt with high affinity. In these and similar situations, the exquisite selectivity of α-CtxArIB-[V11L,V16D] for α7 subtype nAChRs could be invaluable.

In addition to increased selectivity for α7 nAChRs compared to α-Bgt, α-CtxArIB[V11L,V16D] also exhibits notably faster kinetics. The calculated k_{off} (0.128 min^{-1}; see Figure 4) corresponds to a dissociation $t_{1/2}$ of 5.4 min. If eq 2b is solved for *t*, this indicates a 50% relief from functional blockade by a saturating peptide concentration (all five sites blocked) of approximately 16 min. In contrast, [^{125}I]α-Bgt dissociates from solubilized rat cortical (presumably α7 subtype) nAChRs with a $t_{1/2}$ of 15.6 h (*44*). If it is assumed that α-Bgt also blocks five sites on the α7 nAChR, this would correspond to 46 h for a 50% recovery from a saturating blockade. The exceptionally slow off rate of α-Bgt may be useful if essentially irreversible labeling or blockade is required. However, α-CtxArIB[V11L,V16D] offers the possibility of inducing a reversible and very specific blockade of α7 nAChRs. Further, if a radiolabeled version of α-CtxArIB[V11L,V16D] could be made, it would enable true equilibrium binding experiments to be performed, something that is impractical with [^{125}I]α-Bgt.

α-CtxArIB[V11L,V16D] is, in itself, a useful probe. In addition, it completes a set of peptides that may be used together to differentiate previously hard-to-distinguish nAChR subtypes. A variety of muscle (α1) subtype nAChR-specific peptides have been described. For example, α-CtxMI selectively blocks the α1β1γδ nAChR and has 10000-fold selectivity for the α/δ vs the α/γ subunit interface in mammalian receptors (*45*). αA-CtxOIVB selectively blocks the fetal α1β1γδ vs adult α1β1εδ muscle nAChR subtype (*46*), while Waglerin-1 shows the opposite selectivity (*47*), although it may also exert effects on multiple GABA(A) receptor subtypes (*48*). α3β2* and α6β2* nAChRs are both recognized by α-CtxMII but may be distinguished using α-CtxMII[H9A,L15A], which has 2020-fold greater affinity at α6β2* than α3β2* nAChRs (*17*). α-CtxArIB[V11L,-V16D] is highly selective for α7 nAChRs, and α9α10 subtype nAChRs are specifically recognized by α-CtxRgIA (*49*).

ACKNOWLEDGMENT

We thank A. B. Elgoyhen for the kind gift of α9 and α10 nAChR subunit clones.

NOTE ADDED AFTER ASAP PUBLICATION

This paper published ASAP on May 12, 2007 with a typographical error in the α7 selective conotoxin analogue. The correct version was reposted on May 22, 2007.

REFERENCES

1. Wonnacott, S. (1997) Presynaptic nicotinic ACh receptors, *Trends Neurosci. 20*, 92−98.
2. Lindstrom, J. M. (2003) Nicotinic acetylcholine receptors of muscles and nerves: comparison of their structures, functional roles, and vulnerability to pathology, *Ann. N.Y. Acad. Sci. 998*, 41−52.
3. Clarke, P. B. (1992) The fall and rise of neuronal alpha-bungarotoxin binding proteins, *Trends Pharmacol. Sci. 13*, 407−413.
4. Chen, D., and Patrick, J. W. (1997) The alpha-bungarotoxin-binding nicotinic acetylcholine receptor from rat brain contains only the alpha7 subunit, *J. Biol. Chem. 272*, 24024−24029.
5. Schoepfer, R., Conroy, W. G., Whiting, P., Gore, M., and Lindstrom, J. (1990) Brain α-bungarotoxin binding proteins cDNAs and MAbs reveal subtypes of this branch of the ligand-gated ion channel gene superfamily, *Neuron 5*, 35−48.
6. Séguéla, P., Wadiche, J., Dineley-Miller, K., Dani, J. A., and Patrick, J. W. (1993) Molecular cloning, functional properties, and distribution of rat brain α_7: a nicotinic cation channel highly permeable to calcium, *J. Neurosci. 13*, 596−604.

7. Gotti, C., Hanke, W., Maury, K., Moretti, M., Ballivet, M., Clementi, F., and Bertrand, D. (1994) Pharmacology and biophysical properties of α7 and α7-α8 α-bungarotoxin receptor subtypes immunopurified from the chick optic lobe, *Eur. J. Neurosci. 6*, 1281−1291.
8. Elgoyhen, A. B., Vetter, D. E., Katz, E., Rothlin, C. V., Heinemann, S. F., and Boulter, J. (2001) alpha10: a determinant of nicotinic cholinergic receptor function in mammalian vestibular and cochlear mechanosensory hair cells, *Proc. Natl. Acad. Sci. U.S.A. 98*, 3501−3506.
9. Davies, A. R., Hardick, D. J., Blagbrough, I. S., Potter, B. V., Wolstenholme, A. J., and Wonnacott, S. (1999) Characterisation of the binding of [^{3}H]methyllycaconitine: a new radioligand for labelling alpha 7-type neuronal nicotinic acetylcholine receptors, *Neuropharmacology 38*, 679−690.
10. Salminen, O., Whiteaker, P., Grady, S. R., Collins, A. C., McIntosh, J. M., and Marks, M. J. (2005) The subunit composition and pharmacology of alpha-conotoxin MII-binding nicotinic acetylcholine receptors studied by a novel membrane-binding assay, *Neuropharmacology 48*, 696−705.
11. Klink, R., de Kerchove, d'Exaerde, A., Zoli, M., and Changeux, J. P. (2001) Molecular and physiological diversity of nicotinic acetylcholine receptors in the midbrain dopaminergic nuclei, *J. Neurosci. 21*, 1452−1463.
12. Mogg, A. J., Whiteaker, P., McIntosh, J. M., Marks, M., Collins, A. C., and Wonnacott, S. (2002) Methyllycaconitine is a potent antagonist of alpha-conotoxin-MII-sensitive presynaptic nicotinic acetylcholine receptors in rat striatum, *J. Pharmacol. Exp. Ther. 302*, 197−204.
13. Baker, E. R., Zwart, R., Sher, E., and Millar, N. S. (2004) Pharmacological properties of α9α10 nicotinic acetylcholine receptors revealed by heterologous expression of subunit chimeras, *Mol. Pharmacol. 65*, 453−460.
14. Dutertre, S., and Lewis, R. J. (2004) Computational approaches to understand alpha-conotoxin interactions at neuronal nicotinic receptors, *Eur. J. Biochem. 271*, 2327−2334.
15. Terlau, H., and Olivera, B. M. (2004) *Conus* venoms: a rich source of novel ion channel-targeted peptides, *Physiol. Rev. 84*, 41−68.
16. Quiram, P. A., McIntosh, J. M., and Sine, S. M. (2000) Pairwise interactions between neuronal α7 acetylcholine receptors and α-conotoxin PnIB, *J. Biol. Chem. 275*, 4889−4896.
17. McIntosh, J. M., Azam, L., Staheli, S., Dowell, C., Lindstrom, J. M., Kuryatov, A., Garrett, J. E., Marks, M. J., and Whiteaker, P. (2004) Analogs of α-conotoxin MII are selective for α6-containing nicotinic acetylcholine receptors, *Mol. Pharmacol. 65*, 944−952.
18. Azam, L., Dowell, C., Watkins, M., Stitzel, J. A., Olivera, B. M., and McIntosh, J. M. (2005) Alpha-conotoxin BuIA, a novel peptide from *Conus bullatus*, distinguishes among neuronal nicotinic acetylcholine receptors, *J. Biol. Chem. 280*, 80−87.
19. Gerzanich, V., Anand, R., and Lindstrom, J. (1994) Homomers of α8 and α7 subunits of nicotinic acetylcholine receptors exhibit similar channel but contrasting binding site properties, *Mol. Pharmacol. 45*, 212−220.
20. Jacobsen, R., Yoshikami, D., Ellison, M., Martinez, J., Gray, W. R., Cartier, G. E., Shon, K. J., Groebe, D. R., Abramson, S. N., Olivera, B. M., and McIntosh, J. M. (1997) Differential targeting of nicotinic acetylcholine receptors by novel αA-conotoxins, *J. Biol. Chem. 272*, 22531−22537.
21. Marks, M. J., Smith, K. W., and Collins, A. C. (1998) Differential agonist inhibition identifies multiple epibatidine binding sites in mouse brain, *J. Pharmacol. Exp. Ther. 285*, 377−386.
22. Gotti, C., Moretti, M., Clementi, F., Riganti, L., McIntosh, J. M., Collins, A. C., Marks, M. J., and Whiteaker, P. (2005) Expression of nigrostriatal alpha 6-containing nicotinic acetylcholine receptors is selectively reduced, but not eliminated, by beta 3 subunit gene deletion, *Mol. Pharmacol. 67*, 2007−2015.
23. Whiteaker, P., McIntosh, J. M., Luo, S., Collins, A. C., and Marks, M. J. (2000) ^{125}I-a-Conotoxin MII identifies a novel nictonic acetylcholine receptor population in mouse brain, *Mol. Pharmacol. 57*, 913−925.
24. Whiteaker, P., Marks, M. J., Grady, S. R., Lu, Y., Picciotto, M. R., Changeux, J.-P., and Collins, A. C. (2000) Pharmacological and null mutation approaches reveal nicotinic receptor diversity, *Eur. J. Pharmacol. 393*, 123−135.
25. Santos, A. D., McIntosh, J. M., Hillyard, D. R., Cruz, L. J., and Olivera, B. M. (2004) The A-superfamily of conotoxins: structural and functional divergence, *J. Biol. Chem. 279*, 17596−17606.
26. Nicke, A., Loughnan, M. L., Millard, E. L., Alewood, P. F., Adams, D. J., Daly, N. L., Craik, D. J., and Lewis, R. J. (2003) Isolation, structure and activity of GID, a novel 4/7α-conotoxin with an extended N-terminal sequence, *J. Biol. Chem. 278*, 3137−3144.
27. Mergler, M., and Dick, F. (2005) The aspartimide problem in Fmoc-based SPPS. Part III, *J. Pept. Sci. 11*, 650−657.
28. Millard, E. L., Daly, N. L., and Craik, D. J. (2004) Structure-activity relationships of α-conotoxins targeting neuronal nicotinic acetylcholine receptors, *Eur. J. Biochem. 271*, 2320−2326.
29. Luo, S., Nguyen, T. A., Cartier, G. E., Olivera, B. M., Yoshikami, D., and McIntosh, J. M. (1999) Single-residue alteration in α-conotoxin PnIA switches its nAChR subtype selectivity, *Biochemistry 38*, 14542−14548.
30. Whiteaker, P., Jimenez, M., McIntosh, J. M., Collins, A. C., and Marks, M. J. (2000) Identification of a novel nicotinic binding site in mouse brain using [^{125}I]-epibatidine, *Br. J. Pharmacol. 131*, 729−739.
31. Palma, E., Bertrand, S., Binzoni, T., and Bertrand, D. (1996) Neuronal nicotinic α7 receptor expressed in *Xenopus* oocytes presents five putative binding sites for methyllycaconitine, *J. Physiol. (London) 491*, 151−161.
32. Celie, P. H., Kasheverov, I. E., Mordvintsev, D. Y., Hogg, R. C., van Nierop, P., van Elk, R., van Rossum-Fikkert, S. E., Zhmak, M. N., Bertrand, D., Tsetlin, V., Sixma, T. K., and Smit, A. B. (2005) Crystal structure of nicotinic acetylcholine receptor homolog AChBP in complex with an alpha-conotoxin PnIA variant, *Nat. Struct. Mol. Biol. 12*, 582−588.
33. Corringer, P. J., Le Novere, N., and Changeux, J.-P. (2000) Nicotinic receptors at the amino acid level, *Annu. Rev. Pharmacol. Toxicol. 40*, 431−458.
34. Cartier, G. E., Yoshikami, D., Gray, W. R., Luo, S., Olivera, B. M., and McIntosh, J. M. (1996) A new a-conotoxin which targets α3β2 nicotinic acetylcholine receptors, *J. Biol. Chem. 271*, 7522−7528.
35. Kuryatov, A., Olale, F., Cooper, J., Choi, C., and Lindstrom, J. (2000) Human a6 AChR subtypes: subunit composition, assembly and pharmacological responses, *Neuropharmacology 39*, 2570−2590.
36. McIntosh, J. M., Plazas, P. V., Watkins, M., Gomez-Casati, M. E., Olivera, B. M., and Elgoyhen, A. B. (2005) A novel alpha-conotoxin, PeIA, cloned from Conus pergrandis, discriminates between rat alpha9alpha10 and alpha7 nicotinic cholinergic receptors, *J. Biol. Chem. 280*, 30107−30112.
37. Alkondon, M., Pereira, E. F. R., Wonnacott, S., and Albuquerque, E. X. (1992) Blockade of nicotinic currents in hippocampal neurons defines methyllycaconitine as a potent and specific receptor antagonist, *Mol. Pharmacol. 41*, 802−808.
38. Wonnacott, S., Albuquerque, E. X., and Bertrand, D. (1993) Methyllycaconitine: a new probe that discriminates between nicotinic acetylcholine receptor subclasses, *Methods Neurosci. 12*, 263−275.
39. Morley, B. J., Li, H. S., Hiel, H., Drescher, D. G., and Elgoyhen, A. B. (1998) Identification of the subunits of the nicotinic cholinergic receptors in the rat cochlea using RT-PCR and in situ hybridization, *Brain Res. Mol. Brain Res. 53*, 78−87.
40. Haberberger, R. V., Bernardini, N., Kress, M., Hartmann, P., Lips, K. S., and Kummer, W. (2004) Nicotinic acetylcholine receptor subtypes in nociceptive dorsal root ganglion neurons of the adult rat, *Auton. Neurosci. 113*, 32−42.
41. Nguyen, V. T., Ndoye, A., and Grando, S. A. (2000) Novel human alpha9 acetylcholine receptor regulating keratinocyte adhesion is targeted by *Pemphigus vulgaris* autoimmunity, *Am. J. Pathol. 157*, 1377−1391.
42. Peng, H., Ferris, R. L., Matthews, T., Hiel, H., Lopez-Albaitero, A., and Lustig, L. R. (2004) Characterization of the human nicotinic acetylcholine receptor subunit alpha (alpha) 9 (CHRNA9) and alpha (alpha) 10 (CHRNA10) in lymphocytes, *Life Sci. 76*, 263−280.
43. Martyn, J. A., and Richtsfeld, M. (2006) Succinylcholine-induced hyperkalemia in acquired pathologic states: etiologic factors and molecular mechanisms, *Anesthesiology 104*, 158−169.
44. Salvaterra, P. M., and Mahler, H. R. (1976) Nicotinic acetylcholine receptor from rat brain. Solubilization, partial purification, and characterization, *J. Biol. Chem. 251*, 6327−6334.
45. Sine, S. M., Kreienkamp, H.-J., Bren, N., Maeda, R., and Taylor, P. (1995) Molecular dissection of subunit interfaces in the acetylcholine receptor: identification of determinants of α-conotoxin MI selectivity, *Neuron 15*, 205−211.
46. Teichert, R. W., Rivier, J., Torres, J., Dykert, J., Miller, C., and Olivera, B. M. (2005) A uniquely selective inhibitor of the

mammalian fetal neuromuscular nicotinic acetylcholine receptor, *J. Neurosci. 25*, 732−736.
47. McArdle, J. J., Lentz, T. L., Witzemann, V., Schwarz, H., Weinstein, S. A., and Schmidt, J. J. (1999) Waglerin-1 selectively blocks the epsilon form of the muscle nicotinic acetylcholine receptor, *J. Pharmacol. Exp. Ther. 289*, 543−550.
48. Ye, J. H., Ren, J., and McArdle, J. J. (1999) Waglerin-1 inhibits GABA(A) current of neurons in the nucleus accumbens of neonatal rats, *Brain Res. 837*, 29−37.
49. Ellison, M., Haberlandt, C., Gomez-Casati, M. E., Watkins, M., Elgoyhen, A. B., McIntosh, J. M., and Olivera, B. M. (2006) Alpha-RgIA: a novel conotoxin that specifically and potently blocks the alpha9alpha10 nAChR, *Biochemistry 45*, 1511−1517.
50. Yum, L., Wolf, K. M., and Chiappinelli, V. A. (1996) Nicotinic acetylcholine receptors in separate brain regions exhibit different affinities for methyllycaconitine, *Neuroscience 72*, 545−555.
51. McIntosh, J. M., Dowell, C., Watkins, M., Garrett, J. E., Yoshikami, D., and Olivera, B. M. (2002) α-Conotoxin GIC from *Conus geographicus*, a novel peptide antagonist of nicotinic acetylcholine receptors, *J. Biol. Chem. 277*, 33610−33615.

BI7004202